

Filamentous carbons as a support for heteropoly acid

M.N. Timofeeva*, M.M. Matrosova, T.V. Reshetenko, L.B. Avdeeva, A.A. Budneva,
A.B. Ayupov, E.A. Paukshtis, A.L. Chuvilin, A.V. Volodin, V.A. Likholobov

Institute of Catalysis, Novosibirsk 630090, Russia

Received 13 February 2002; received in revised form 11 March 2002; accepted 1 October 2003

Abstract

For an heterogenization, different kinds of catalytic filamentous carbons (CFC) were used as a support for some heteropoly acids (HPAs): $H_6P_2W_{21}O_{71}(H_2O)_3(P_2W_{21})$, $H_6As_2W_{21}O_{69}(H_2O)(As_2W_{21})$, Dawson type $\alpha-H_6P_2W_{18}O_{62}(P_2W_{18})$ and Keggin type $H_3PW_{12}O_{40}(PW)$. The support properties, which affect the interaction between HPAs and supports were studied. Concentration of Brønsted acidic sites in PW and PW/support was determined from the ESR studies of the stable nitroxyl radical (4-hydroxy-2,2',6,6'-tetramethylpiperidin-*N*-oxyl (TEMPOL)) adsorbed from hexane. The reaction of 2,6-di-*tert*-butyl-4-methylphenol (DMBP) with toluene as *tert*-butyl acceptors was studied using bulk and supported PW and P_2W_{18} . It was found that P_2W_{18} was more active than PW. It was shown that catalytic activities of HPAs supported on SiO_2 and CFC were approximately equal. The activity of the surface protons in HPA/support increased monotonically as the total HPA loading increased, reaching a maximum for the bulk HPA.

© 2003 Elsevier B.V. All rights reserved.

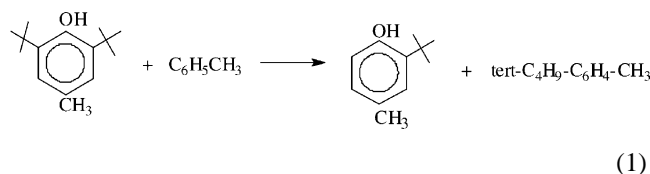
Keywords: Heteropoly acid; Keggin-type structure; Dawson-type structure; Catalytic filamentous carbon; Adsorption; De-*tert*-butylation of 2,6-di-*tert*-butyl-4-methylphenol; Acidity; ESR; TEMPOL

1. Introduction

Heteropoly acids (HPA) are strong Brønsted acids, which are used widely as homogeneous and heterogeneous acid catalysts [1,2]. The higher catalytic activity showed by these systems as compared with that of bulk HPAs motivates the lively interest in heterogenization of HPA on the support surface [3–5]. Moreover, the supported systems are of practical importance as the catalytic activity in some reactions is correlated with the specific surface area.

Many porous materials (SiO_2 , carbon, Al_2O_3 , and MgF_2) [3–8] are used as supports for HPAs. At present there is a huge variety of carbons with different structure. Recently, researchers, which work in fields of catalysis and adsorption, give much attention to carbon–carbonaceous composite materials, such as Sibunit and catalytic filamentous carbons (CFC) produced by decomposition of gaseous hydrocarbons over the iron-group catalysts at 700–900 K [9,10]. Morphology and structure of growing CFC filaments are dictated by the catalyst composition [9]. Most of these materials are designed for adsorption and catalysis [4,11,12].

In this paper, we describe adsorption and desorption of HPA ($H_3PW_{12}O_{40}$, $H_6P_2W_{18}O_{62}$, $H_6P_2W_{21}O_{71}$, $H_6As_2W_{21}O_{69}$) on CFC. We study also the influence of the structure of CFC and their specific surface area on strength and amount of HPA adsorbed. Lastly, we compare the catalytic activity of the PW/CFC-2, P_2W_{18} /CFC-2 and PW/ SiO_2 in the reaction of 2,6-di-*tert*-butyl-4-methylphenol (DMBP) with toluene as *tert*-butyl acceptors.



2. Experimental

2.1. Materials

$H_3PW_{12}O_{40} \cdot 15H_2O$ of chemical purity grade was twice recrystallized from water. $H_6P_2W_{21}O_{71}(H_2O)_3 \cdot 29H_2O$, $\alpha-H_6P_2W_{18}O_{62} \cdot 17H_2O$, $H_5PW_{11}ZrO_{40} \cdot 16H_2O \cdot TiO_{40} \cdot 14H_2O$ and H_5PW_{11} were synthesized by electrochemical meth-

* Corresponding author.

E-mail address: timofeeva@catalysis.nsk.su (M.N. Timofeeva).

Table 1
The main characteristic of CFC and PW/CFC

Sample	The main characteristics				The adsorption characteristic a_{\max} , mg g ⁻¹		H ⁺ ^a ($\mu\text{mol g}^{-1}$)	Catalytic tests ^b	
	S_{BET} (m ² g ⁻¹)	ΣV_{pore} (cm ³ g ⁻¹)	D_{micro} (Å)	Metal (wt.%)	H ₂ O	MeOH		$10^3 k_{\text{HPA}}$ (s ⁻¹ mol ⁻¹)	k_{H^+} (s ⁻¹ mol ⁻¹)
CFC-1	100	0.3	100	Ni < 1	79	18	10	0	0
CFC-2	179	0.4	80–90	Ni, Cu ~ 0.5	352	140	9	0	0
8% PW/CFC-1	100	–	–	–	–	–	37	0.9	24
8% PW/CFC-2	179	–	–	–	–	–	24	0.9	38

S_{BET} is the surface area, D_{micro} the diameter of micropore, and a_{\max} the amount of PW adsorbed on CFC.

^a The number of acidic centers were determined by TEMPOL titration.

^b Catalytic activity of PW/support (0.8 wt.%) in reaction (1) ([DBMP]/[PhMe] = 1/30, 50 °C).

ods [13–15]. H₆As₂W₂₁O₆₉(H₂O)·17H₂O was synthesized according to the method described in [16]. The purity of HPA was controlled by ³¹P and ¹¹B NMR on an MSL-400 Bruker instrument. The amount of hydrated water in HPA was determined from the weight loss after calcination at 500 °C.

2,6-di-*tert*-butyl-4-methylphenol DBMP (97%) of chemical purity grade was twice recrystallized from hexane in order to obtain reproducible results. Toluene of chemical purity grade was used without further purification.

HPA/SiO₂ and HPA/CFC catalysts were prepared by impregnation of SiO₂ (IKT-04–6, surface area 360 m² g⁻¹, pore volume 1.2 cm³ g⁻¹, mean pore radius 170 Å, particle size 0.1–0.2 mm) and CFC (main characteristics of carbon are shown in the Table 1) with an aqueous (or MeOH) solution and dried overnight in a desiccator. Before tests, each catalyst was calcined at 150 °C for 2 h. BET specific surface area, S_{BET} , was determined by the nitrogen thermodesorption method.

2.2. Impregnation procedure

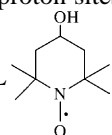
Experimental studies of HPA impregnation were carried out at 20 °C in a glass thermostat (± 0.1 °C) vessel under stirring. The reactor was loaded with 1 g support pre-activated by calcination at 120 °C for 1 h in vacuum (10 Pa), 10 ml of HPA-solution (10–100 mmol l⁻¹). At regular intervals, the samples of this mixture were taken, and solid and the solution were centrifuged for their spectrophotometric analysis (Specord UV–VIS M-40 in constant-temperature cells, $\nu = 32000\text{--}42000$ cm⁻¹).

The quantity of surface protons was determined by the following procedure: 1 g of samples was heated at 120 °C for 2 h in vacuum (10 Pa) and 2 ml diphenylamine (21.57 mmol l⁻¹) ($\text{p}K_{\text{a}} = +0.78$) in benzene was added. The equilibrium in system at 20 °C was reached in an hour and kept for 24 h. The quantity of the surface protons (Q_{SP}) were measured by UV–Vis analysis ($\nu = 220\text{--}370$ nm) and were calculated as.

$$Q_{\text{SP}} = \frac{Q_{\text{AD}} - Q_{\text{ADS}}}{m}$$

where Q_{AD} and Q_{ADS} are the quantity of adsorbed diphenylamine (μmol) onto HPA/support and support respectively, and m is the weight of sample HPA/support (g).

The amount of proton sites were determined from curves

given by TEMPOL  on solid samples (error $\pm 15\%$).

Equilibrium concentration of TEMPOL in hexane solution was measured by ESR.

ESR spectra (room temperature) were recorded at 9.5 GHz on a ERS-221 spectrometer in glass cylindrical tubes ($d = 4$ mm), these spectra were quantified by double integration, the concentration of TEMPOL was calculated after calibration procedure (error $\pm 10\%$). Before measurement, the samples were heated in oxygen atmosphere at 200 °C for 2 h.

2.3. Products and kinetics

Reaction (1) was carried out at 50 °C in a glass thermostatted (± 0.1 °C) vessel equipped with a stirrer and a reflux condenser. DBMP, toluene ([DBMP]/[PhMe] = 1/30 mol mol⁻¹ and catalyst (0.8 wt.% total content in the reaction mixture) were charged in the reactor. To eliminate diffusion restrictions, catalyst particles as small as 0.1–0.2 mm in size were used and the mixture was vigorously stirred (500 rpm). The reaction mixture was sampled periodically. The reaction in the taken sample was stopped by treating with a mixture of toluene and aqueous benzidine.

Reaction products were analyzed by GLC: 2 m column packed with 5% SE-30 on Chromosorb W, 150–200 °C (10 °C min⁻¹) and decane as internal standard.

First-order rate constant, k , was calculated from the equation $\ln[\text{DBMP}]/[\text{DBMP}]_0 = -k\tau$, the conversion of DBMP did not exceed 50%.

2.4. Instrumental measurements

IR-spectra were recorded on a FTIR-8300 Shimadzu spectrometer (700–1800 cm⁻¹). The samples of PW/CFC-2 were sprayed on NaCl plate.

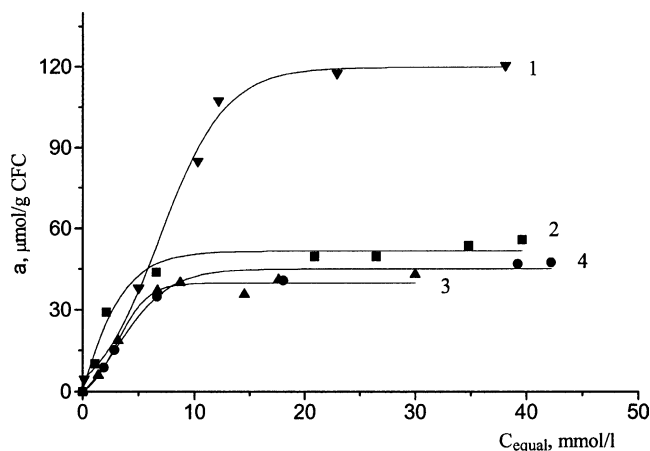


Fig. 1. Adsorption isotherms of HPAs on CFC-2 from aqueous solutions. (1): $\text{H}_3\text{PW}_{12}\text{O}_{40}$; (2): $\text{H}_6\text{P}_2\text{W}_{21}\text{O}_{71}\cdot(\text{H}_2\text{O})_3$; (3): $\text{H}_6\text{As}_2\text{W}_{21}\text{O}_{69}\cdot(\text{H}_2\text{O})$; (4): $\text{H}_6\text{P}_2\text{W}_{18}\text{O}_{62}$.

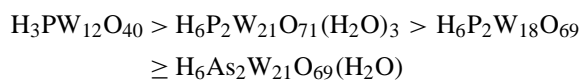
BET specific surface area was measured. Pore structures were determined from nitrogen adsorption isotherms (77 K) in a Micrometrics ASAP 2400 instrument. Pore size distributions were calculated from the desorption branch of isotherms in the range of capillary-condensation hysteresis by Broeckhoff and De Boer method.

Dispersion of HPA molecules on the external surface of carbon filaments was determined using a JEM-2010 scanning electron microscope.

3. Results

3.1. Adsorption of HPA onto CFC

Adsorption of different tungsten-containing heteropolyacids on CFC were studied. Adsorption isotherms are shown in Fig. 1 and Tables 1 and 2. It was established that the adsorption of heteropolyacids from aqueous solution is irreversible. The adsorbed amount of HPA (a_{max}) decreases in the series (Table 2):



Due to their small sizes, HPA of Keggin structure $\text{H}_3\text{PW}_{12}\text{O}_{40}$ was adsorbed to a greater extent than HPA of other type. The quantity of adsorbed HPA is solvent

Table 2
The adsorbed amount of HPA from aqueous solution on CFC-2

HPA	a_{max}	
	(mg g^{-1})	($\mu\text{mol g}^{-1}$)
$\text{H}_3\text{PW}_{12}\text{O}_{40}$	352	122
$\text{H}_6\text{P}_2\text{W}_{21}\text{O}_{71}(\text{H}_2\text{O})_3$	252	50
$\text{H}_6\text{As}_2\text{W}_{21}\text{O}_{69}(\text{H}_2\text{O})$	167	35
$\text{H}_6\text{P}_2\text{W}_{18}\text{O}_{62}$	183	42

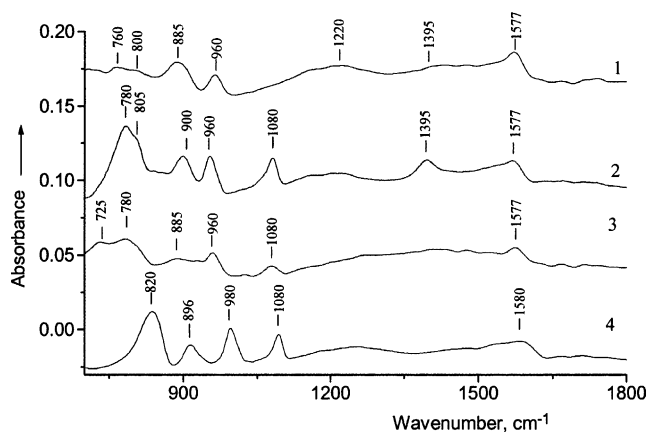


Fig. 2. FT-IR spectra of supported HPAs on CFC-2. (1): 5% $\text{As}_2\text{W}_{21}/\text{CFC-2}$; (2): 5% $\text{P}_2\text{W}_{18}/\text{CFC-2}$; (3): 5% $\text{P}_2\text{W}_{21}/\text{CFC-2}$; (4): 20% $\text{PW}/\text{CFC-2}$.

dependent (Table 1). Adsorption from MeOH decreases as the polarity of solvent increases, and, more importantly, the adsorbed quantity depends on the competitive adsorption of solvent molecules and molecules of HPA on the outer surface of CFC.

IR spectra of tungsten-containing heteropoly acids supported on CFC-2 (Fig. 2) show that the HPA structure does not change during adsorption. For example, bands at 820, 896, 980 and 1077 cm^{-1} attributed to bulk $\text{H}_3\text{PW}_{12}\text{O}_{40}$ are observed in the spectrum of 20% $\text{PW}/\text{CFC-2}$. For 5% $\text{P}_2\text{W}_{18}/\text{CFC-2}$, there are bands at 780, 805, 900, 960, 1080 cm^{-1} that are observed in the spectrum of $\text{H}_6\text{P}_2\text{W}_{18}\text{O}_{62}$ [16]. The absorption bands at 725, 780, 885, 960, 1080 cm^{-1} for 5% $\text{P}_2\text{W}_{21}/\text{CFC-2}$ and at 760, 800, 885, 960 cm^{-1} for 5% $\text{As}_2\text{W}_{21}/\text{CFC-2}$ are observed in the spectra of individual HPAs [16]. As shown in Fig. 2, in region of 1200–1800 cm^{-1} the broad bands are observed, they can be attributed to the surface groups of carbon (lactone or carboxyl groups and others) [17].

Correlation between textural properties of CFCs and adsorption amount a_{max} was observed (Table 1). Fig. 3 is a basic scheme of structure of CFC filaments. Catalyst CFC-1 filaments obtained with Ni is built up from cones put into

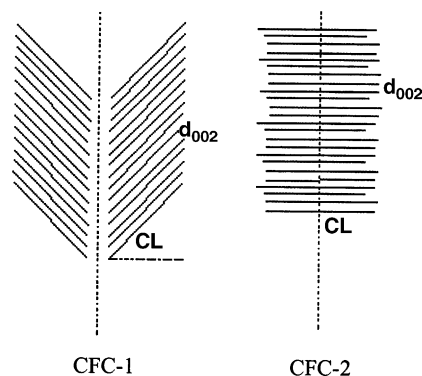


Fig. 3. Schematic representation of CFC texture.

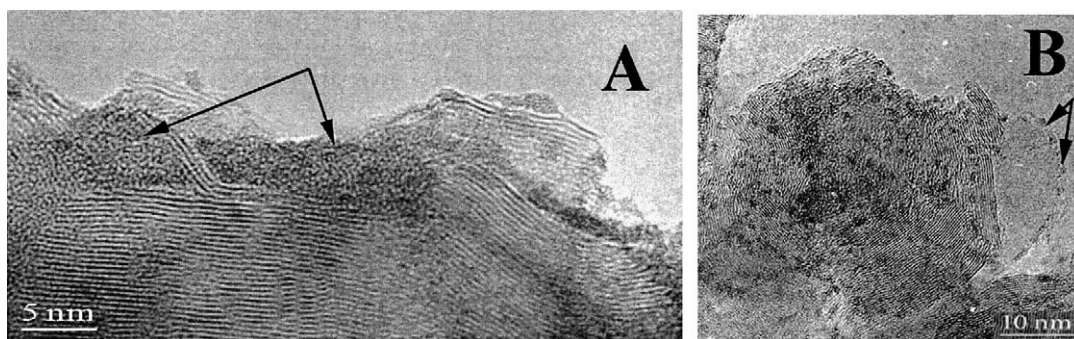
Fig. 4. Electron micrographs of $H_3PW_{12}O_{40}$ supported on CFC-2.

Table 3

The number of surface acid sites at the CFC-2 surface

PW (PW + CFC-2) ($g\ g^{-1}$)	H^+ ($\mu mol\ g^{-1}$) ^a					Theory ^c
	Theory ^b	<i>n</i> -C ₄ H ₉ NH ₂	C ₅ H ₅ N	(C ₆ H ₅) ₂ NH	TEMPOL	
8	28	14	24	24	24	28
20	69	–	28	31	–	69
26	90	–	52	31	–	90
40	139	139	45	24	–	139
75	260	156	38	10	–	50
Bulk	347	215	128	7	4	5

^a The number of acidic centers were determined by different methods.^b Total number of acid sites is calculated from the weight of PW.^c Total number of acid sites is calculated from surface area of catalyst and the area occupied by an PW anion ($100\ \text{\AA}^2$) [1].

one another, each cone being a rolled-up graphite plane with an angle of $45\text{--}60^\circ$ at the cone top. CFC-2 is obtained with Cu–Ni catalysts [18]. From the microstructure of CFC, one can suppose that low adsorption centers are typical of CFC-1 and CFC-2. The distinction between these CFC in the quantity of adsorbed HPA can be attributed to specific surface area, total volume pore, the structure and concentration of the adsorption centers on CFC surface. Therefore, adsorption centers in CFC-1 are localized on edges of graphite layers on a filament surface, while the adsorption centers of CFC-2 may also be localized at defects of graphite package in filaments.

SEM data (Fig. 4) show that PW molecules are adsorbed on the outer surface of filamentous carbon. Individual HPA molecules penetrated into holes, localizing at defect of packages of graphite sheets in filaments, and become new centers for further adsorption (Fig. 4A). Various HPA forms are observed on the CFC-2 surface: individual molecules less than $20\ \text{\AA}$ in size (Fig. 4B), clusters of approximately $50\ \text{\AA}$ in size (Fig. 4B), and large crystallites larger than $150\ \text{\AA}$ (Fig. 4A). The distribution depends on the HPA loading. The formation of three form of finely dispersed HPA species on SiO₂ and active carbon surface was observed earlier while the large crystals was only observed on carbon film [6].

3.2. Surface acidity of $H_3PW_{12}O_{40}/\text{support}$

The determined number of surface acid sites at the SiO₂ and CFC surface are shown in Tables 3–5. It was establish

Table 4

Catalytic activity of PW/SiO₂ (0.8 wt.%) in reaction (1) ([DBMP]/[PhMe] = 1/30, 50 °C)

PW (PW + SiO ₂) ($g\ g^{-1}$)	S_{BET} ($m^2\ g^{-1}$)	H^+ ^a ($\mu mol\ g^{-1}$)	$10^3\ k_{HPA}$ ($s^{-1}\ mol^{-1}$)	k_{H^+} ($s^{-1}\ mol^{-1}$)
0.05	344	10	0	0
0.10	344	25	0.1	4
0.15	344	–	0.5	–
0.20	344	25	1.0	41
0.25	344	25	1.1	44
0.30	280	21	1.0	48
0.40	230	21	1.0	48
0.60	100	–	0.9	–
0.75	30	10	0.9	90
Bulk	3	7	0.8	114

^a Diphenilamine was used as an indicator.

Table 5

Catalytic activity of PW/CFC-2 (0.8 wt.%) in reaction (1) ([DBMP]/[PhMe] = 1/30, 50 °C)

PW (PW + CFC-2) ($g\ g^{-1}$)	S_{BET} ($m^2\ g^{-1}$)	H^+ ^a ($\mu mol\ g^{-1}$)	$10^3\ k_{HPA}$ ($s^{-1}\ mol^{-1}$)	k_{H^+} ($s^{-1}\ mol^{-1}$)
0.05	160	–	0.8	–
0.08	160	24	0.9	38
0.11	150	27	1.0	37
0.20	150	31	1.1	35
0.26	149	31	1.1	35
0.40	100	24	1.1	52
0.75	30	10	0.8	80
Bulk	3	7	0.8	114

^a Diphenilamine was used as indicator.

that when $n\text{-C}_4\text{H}_9\text{NH}_2$ and $\text{C}_5\text{H}_5\text{N}$ are used as indicators, the number of acidic centers are larger than that calculated from the amount of supported PW, surface area and the area occupied by an PW anion (100 \AA^2) [1] (Table 3). This phenomenon is attributable to adsorption polar molecules (e.g. amines, ethers etc. [1]) on solid HPAs in large amount. $(\text{C}_6\text{H}_5)_2\text{NH}$ with a large steric groups was used for determining the surface acidity. As shown in the Tables 3–5 the number of surface acid sites has only a weak dependence on the amount of supported PW. Such a dependence is attributable to decrease in surface area and concurrent increase of strength of acidic sites with increasing HPA loading.

In recent studies [19,20], we found that nitroxyl radicals TEMPOL can be used for estimation of surface concentration of acidic sites.

Adsorption of TEMPOL on PW, CFC and 8% PW/CFC from hexane was studied (Table 1, and Fig. 5). TEMPOL adsorbed from hexane on bulk PW, CFC and 8% PW/CFC gives L-curve (“Langmuir” type [21]) with the plateau (Fig. 5). The plateau level corresponds to surface concen-

tration of acidic sites. Determined by TEMPOL adsorption, such a concentration for PW is $4 \mu\text{mol g}^{-1}$. As the specific surface area of bulk PW is about $4 \text{ m}^2 \text{ g}^{-1}$, it corresponds to surface density of acid sites $0.6 \text{ site per } 100 \text{ \AA}^2$ and nearest-neighbor separation distance between these sites $\sim 14 \text{ \AA}$. Such distance is about nearest-neighbor separation $\text{PW}_{12}\text{O}_{40}^{3-}$ in bulk PW ($11\text{--}15 \text{ \AA}$) [22].

TEMPOL also adsorbs on CFC-1 and CFC-2 (Fig. 5, curves 2 and 4). Such an adsorption is attributable to the presence of their own acid groups (e.g. carboxylic, lactonic etc.) on the outer surface of these supports [4,11,23]. The concentration of the acid groups on CFC-1 happened to be close to that on CFC-2. However, those acid groups are inactive in catalytic conversions (Table 1).

The concentration of acid sites in supported HPA is higher than in bulk HPA due to higher dispersion of HPA aggregates (Table 1, and Fig. 5, curves 3 and 5) after adsorption on CFC. Due to higher dispersivity of HPA, the concentration of acid sites of 8% PW/CFC-1 is more than that of CFC-2. However, the determined concentration of acid sites in 8% HPA/CFC is lower than expected ($27 \times 3 \mu\text{mol g}^{-1}$), and such a concentration is attributable to the interaction of HPA protons with surface groups of CFC (e.g. $\text{C}\text{--}\text{OH}$ and $\text{C}\text{=}\text{O}$) [23]. This interaction is also corresponds to IR spectra region $800\text{--}1100 \text{ cm}^{-1}$ (Fig. 2). This interaction lead to decrease of specific catalytic activity after supporting on CFC-1 (Table 1).

Results of acidity determining by TEMPOL adsorption are in agreement with DPHA titration. We suppose that this is attributable to similarity of steric and basic properties of these test-molecules.

3.3. Catalytic activity of PW/SiO_2 and HPA/CFC

Rate constants k_{HPA} and k_{H^+} were calculated using the known values of first-order rate constants, k , and the amount of the surface protons for bulk and supported PW, respectively. K_{HPA} is the activity based on the total amount of PW protons in the catalyst, while k_{H^+} is based on the amount of the surface protons. The main results of catalytic tests of PW/SiO_2 and $\text{PW}/\text{CFC-2}$ in the reaction (1) are presented in Tables 4 and 5.

In general, the behavior of k_{HPA} of catalysts ($\text{PW}/(\text{PW} + \text{Support})$) is independent of the support nature (Fig. 6A). The k_{HPA} value increases with $\text{PW}/(\text{PW} + \text{Support})$, reaches a maximum and then tends to decrease. Unusual behavior of k_{HPA} can be accounted for both by monotonic rise of the strength of protons with increasing PW loading and by a decrease in the amount of PW protons on the catalyst surface. When CFC-2 was used as the support, the k_{HPA} value was maximal for 7 wt.% $\text{PW}/\text{support}$. With SiO_2 , the maximal k_{b} value was observed for 25% $\text{PW}/\text{support}$. This distinction may be explained by the difference of surface area of the catalysts (Tables 4 and 5).

In contrast to k_{HPA} , the k_{H^+} value (Fig. 6B) increases monotonically as the acid strength increases with an increase

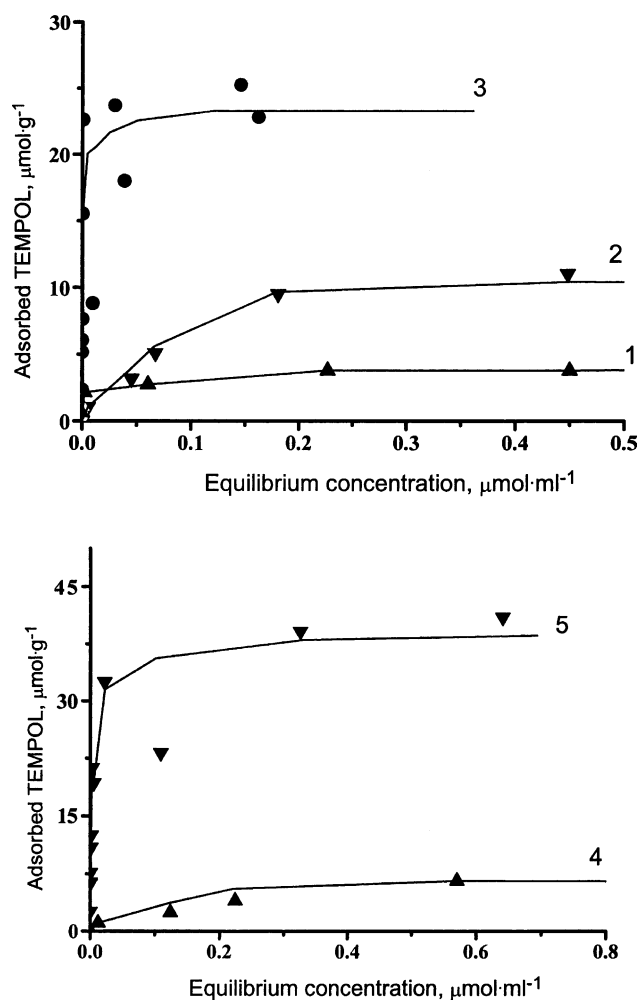


Fig. 5. Adsorption isotherms of TEMPOL on samples from hexane solution on PW and CFC at $25 \text{ }^\circ\text{C}$. (1) $\text{H}_3\text{PW}_{12}\text{O}_{40}$; (2) CFC-2; (3): 8%PW/CFC-2; (4): CFC-1; (5): 8%PW/CFC-1.

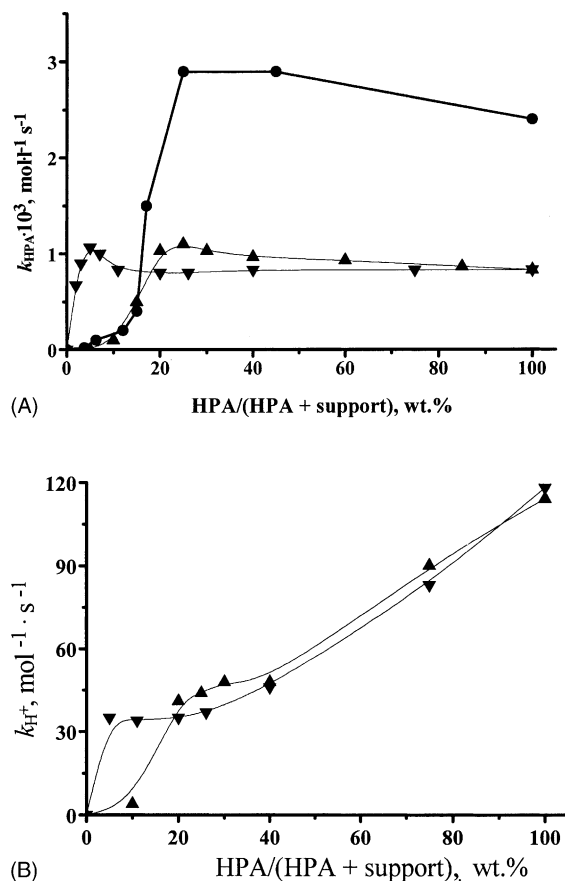


Fig. 6. Dependence of catalytic activity on HPA loading in reaction (1). (A): k_{HPA} represents the activity based on the total amount of $\text{H}_3\text{PW}_{12}\text{O}_{40}$ protons; (B): k_{H^+} is based on the amount of the surface protons. (\blacktriangledown) PW/CFC-2; (\blacktriangle) PW/SiO₂; (\bullet) P₂W₁₈/CFC-2.

in the HPA loading on the support surface. However, the k_{H^+} is far lower in the case of SiO₂ than in the case of CFC-2 at the range of 0 to 20 wt.% PW loading. Therefore, the surface protons of PW/CFC-2 were stronger than the surface protons of PW/SiO₂. At higher PW loading, the amount and strength of surface protons of both supports became approximately equal.

Dependences of k_{HPA} value on the amount of supported of P₂W₁₈ were similar to those observed with PW/(PW + Support) (Tables 5 and 6, and Fig. 6A). The comparative

Table 6
Catalytic activity of P₂W₁₈/CFC-2 (0.8 wt.%) in reaction (1) ([DBMP]/[PhMe] = 1/30, 50 °C)

P ₂ W ₁₈ (P ₂ W ₁₈ +CFC-2) (g g ⁻¹)	10 ³ k_{HPA} (s ⁻¹ mol ⁻¹)
0.04	0.02
0.06	0.1
0.12	0.2
0.15	0.4
0.17	1.5
0.25	2.9
0.45	2.9
1.00	2.4

catalytic activities of P₂W₁₈/CFC-2 and PW/CFC-2 systems show that the catalytic activity was lower for P₂W₁₈/CFC-2 than for PW/CFC-2 at the HPA content below 20 wt.%. This fact indicates that P₂W₁₈ interacts stronger with filamentous carbon supports than PW. But for bulk P₂W₁₈, k_{HPA} was approximately 3 times higher than those of bulk PW₁₂.

The only reaction, gas phase synthesis of MTBE [3], is known now in which the catalytic activity of bulk and supported Dawson-type acid H₆P₂W₁₈O₆₂ compares with that of Keggin-type heteropolyacids (H_nXW₁₂O₄₀, X = P^V, Si^{IV}, Ge^{IV}, B^{III}, Co^{III}). The activity (per unit weight) of P₂W₁₈ is at least 13 times higher than those of PW [3]. At the same time the difference in the activity between P₂W₁₈ and PW was ~ 2.7 times per weight in the homogeneous liquid-phase synthesis of TBME [24]. It also was found that the activity of P₂W₁₈ was considerably enhanced by supporting it on SiO₂ [3]. However the activity (per unit weight) of bulk P₂W₁₈ was lower than that of supported P₂W₁₈. Thus the available data demonstrate that both the acidity of proton sites and the amount of proton sites are among key factors determining the catalytic activity in acidic reactions.

4. Conclusion

The results obtained lead to conclude the following:

1. The structure and the surface area of CFC influence considerably, the strength and amount of HPA adsorbed. The reversible HPA adsorption is observed with CFC-1 and CFC-2.
2. The P₂W₁₈/CFC-2 system, as well as PW/CFC-2 and PW/SiO₂, exhibited high catalytic activity to de-*tert*-butylation of 2,6-di-*tert*-butyl-4-methylphenol.
3. The acidity of supported HPAs depends on the nature of surface species and on the strength of the HPA-support interaction. The activity of surface protons of HPA/support increases monotonically as their acid strength increases with increasing total HPA loading to reach maximum for the bulk HPA.

Acknowledgements

The authors would like to thank Prof. I.V. Kozhevnikov and Dr. G.M. Maksimov for their participation in some of the experiments presented in the paper. This work was financially supported by Russian Foundation for Basic Research (Project No. 03-03-33178).

References

- [1] T. Okuhara, N. Mizuno, M. Misono, Adv. Catal. 41 (1996) 113.
- [2] I.V. Kozhevnikov, Catalysis by polyoxometalates, Catalysis For Fine Chemical Synthesis, Vol. 2., UK, 2002, p. 200.

- [3] S. Shikata, S. Nakata, T. Okuhara, M. Misono, *J. Catal.* 166 (1997) 263.
- [4] M.N. Timofeeva, M.M. Matrosova, G.N. Il'inich, T.V. Reshetenko, L.B. Avdeeva, R.I. Kvon, A.L. Chuvilin, A.A. Budneva, E.A. Paukshtis, V.A. Likholobov, *Kinetika i kataliz.* 44 (5) (2003) 1 (in Russian).
- [5] S. Shikata, S. Nakata, T. Okuhara, M.J. Misono, *Catalysis* 166 (1997) 263.
- [6] S.M. Kulikov, M.N. Timofeeva, I.V. Kozhevnikov, V.I. Zaikovskii, L.I. Plyasova, I.A. Ovsyanikova, *Izvestiya Akademii nauk, ser. khimiya*, 1989, 763 (in Russian).
- [7] L.R. Pizzio, C.V. Caceres, M.N. Blanco, *Appl. Catal. A* 167 (1998) 283.
- [8] M.E. Chimienti, L.R. Pizzio, M.N. Blanco, C.V. Caceres, *Appl. Catal. A* 208 (2001) 7.
- [9] V.A. Likholobov, V.B. Fenelonov, O.G. Okkel, O.V. Goncharova, L.B. Avdeeva, V.I. Zaikovskii, G.G. Kuvshinov, V.A. Semikolenov, V.K. Duplyakin, O.N. Baklanova, G.V. Plaksin, *React. Kinet. Catal. Lett.* 54 (1995) 381.
- [10] V.B. Fenelonov, A.Yu. Derevyankin, L.G. Okkel, L.B. Avdeeva, V.I. Zaikovskii, E.M. Moroz, A.N. Salanov, N.A. Rudina, V.A. Likholobov, Sh.K. Shaikhutdinov, *Carbon* 33 (1997) 1140.
- [11] M.N. Timofeeva, M.M. Matrosova, T.V. Reshetenko, L.B. Avdeeva, E.A. Paukshtis, A.A. Budneva, A.L. Chuvilin, V.A. Likholobov, *Russ. Chem. Bull. Int. Ed.* 51 (2) (2002) 243.
- [12] Yu.A. Ryndin, O.S. Alekseev, P.A. Simonov, V.A. Likholobov, *J. Mol. Catal.* 55 (1989) 109.
- [13] O.M. Kulikova, R.I. Maksimovskaya, S.M. Kulikov, I.V. Kozhevnikov, *Izvestiya Akademii nauk, seriya khimiya*, 1992, 494 (in Russian).
- [14] G.M. Maksimov, R.I. Maksimovskaya, I.V. Kozhevnikov, *Zhurn. neorgan. khimii* 37 (1992) 2279 (in Russian).
- [15] G.Ĭ. Maksimov, R.I. Maksimovskaya, I.V. Kozhevnikov, *Zhurn. neorgan.khimii* 39 (1994) 623 (in Russian).
- [16] *Inorganic Synthesis*, Vol. 27, Wiley, New York, 1990, p. 112.
- [17] W. Yue, X. Ye, X. Yang, X. Wang, W. Chu, Y. Hu, *Ind. Eng. Chem. Res.* 35 (1996) 2546.
- [18] L.B. Avdeeva, O.V. Goncharova, D.I. Kochubey, V.I. Zaikovskii, L.M. Plyasova, B.N. Novgorodov, Sh.K. Shaikhutdinov, *Appl. Catal. A* 141 (1996) 117.
- [19] A.B. Ayupov, G.V. Echevsky, E.A. Paukshtis, D.J. O'Rear, C.L. Kibby, *Stud. Surf. Sci. Catal.*, Vol. 135, Elsevier Science, 2001, 13-p-09.
- [20] M.N. Timofeeva, A.B. Ayupov, A.V. Volodin, E.A. Paukshtis, G.G. Volkova, Yu. E. Pak, Echevsky G.V., *Kinetika i kataliz.* (in Russian), in press.
- [21] C.H. Giles, T.H. MacEvan, S.N. Nakwa, D. Smith, *J. Chem. Soc.* (1960) 3973.
- [22] W.G. Klemperer, C.G. Wall, *Chem. Rev.* 98 (1998) 297.
- [23] W.B. Downs, R.T.K. Baker, *Carbon* 29 (8) (1991) 1173.
- [24] G.M. Maksimov, I.V. Kozhevnikov, *React. Kinet. Catal. Lett.* 39 (1989) 317.